Tellus (2007), 59, 742–754
Printed in Singapore. All rights reserved

TELLUS

Temporal variation of water-soluble ions of free tropospheric aerosol particles over central Japan

By K. OSADA[1]*, M. KIDO[2], C. NISHITA[1], K. MATSUNAGA[1], Y. IWASAKA[3], M. NAGATANI[4] and H. NAKADA[4], [1]*Graduate School of Environmental Studies, Nagoya University, Nagoya, 464-8601, Japan;* [2]*Toyama Prefectural Environmental Science Research Center, Imizu, 939-0363, Japan;* [3]*Kanazawa University, Kanazawa, 920-1192, Japan;* [4]*Solar Terrestrial Environment Laboratory, Nagoya University, Toyokawa, 442-8507, Japan*

(Manuscript received 14 October 2006; in final form 28 May 2007)

ABSTRACT

Free tropospheric aerosol particles were collected at Mt. Norikura (36.1°N, 137.5°E, 2770 m a.s.l.) in Japan during May–October in 2001 and 2002. An automated sequential daily nighttime (00–06 a.m.) sampler collected free tropospheric aerosols. Average, median, *SD*, minimum and maximum concentrations of total ionic weight of the 114 samples were, respectively, 3.9, 2.8, 3.7, 0.2 and 23.2 μg m^{-3}. Transport conditions were analysed using backward air trajectory with precipitation amounts along the trajectory. Results suggest that low aerosol mass concentration causes are (1) descending trajectories and (2) precipitation scavenging during transport without contacting boundary layer atmosphere until arrival. It is suggested that, without precipitation scavenging after entrainment into the free troposphere, aerosol transport from active emissions at the surface enhances mass concentration at Mt. Norikura.

Average concentrations of NO_3^-, non-sea-salt (nss)K^+ and $C_2O_4^{2-}$ are high in March–June and low in winter. The highest average nssSO_4^{2-} concentration occurs in summer; it is high from spring through fall. Seasonal variation of NH_4^+ concentrations resembles that of nssSO_4^{2-}, but the concentrations' molar ratio (NH_4^+/nssSO_4^{2-}) is high (*ca.* 2) in spring and decreases to 1 in winter. Seasonal variation of $NH_4^+ + NH_3$ concentration agrees with that of NH_3 emissions in China.

1. Introduction

Atmospheric aerosol particles in the free troposphere (FT) strongly alter direct and indirect radiation effects in the Earth's atmosphere (Charlson and Heintzenberg, 1995; Andreae, 1995). Submicrometer aerosol particles are produced mainly by gas-to-particle conversion processes in the atmosphere, whereas supermicrometer aerosol particles are formed by disintegration processes of bulk material on the earth's surface (e.g. sea salt and dust; Jaenicke, 1993; Warneck, 1999). Most aerosol particles formed near the ground might remain within the planetary boundary layer (typically several hundred metres to a few kilometres of thickness above the ground, Stull, 2000), but some might be entrained into the FT and transported longer distances. In general, aerosol mass concentrations in the troposphere decrease with increasing altitude (Jaenicke, 1993; Dibb et al., 1996; 1997; 2003; Kline et al., 2004; Inomata et al., 2006; Yoon et al., 2006). Aerosol particles are eventually removed from the atmosphere by precipitation scavenging and by dry processes such as gravitational settling (Warneck, 1999; Seinfeld and Pandis, 2006). For those reasons, vertical and horizontal distributions of aerosol particles in the FT might depend on source intensity, vertical and horizontal transport from the source area, and wet and dry deposition during transport.

Several areas showing high aerosol contents in the atmosphere have been identified by observations from satellite remote sensors (Husar et al., 1997; Kaufman et al., 2002). Among them, East Asia is considered a globally important source area of anthropogenic NO_x, SO_2 and NH_3 gases as well as submicrometer aerosols. In addition, frequent dust storms in spring at dry desert areas (such as the Gobi and Taklamakan Deserts) of East Asia inject enormous quantities of mineral dust particles (yellow sand, or Kosa in Japan) into the FT; they are subsequently transported eastward (Duce et al., 1980; Iwasaka et al., 1983; Uematsu et al., 1983). Along with migration of a synoptic-scale low-pressure system, anthropogenic aerosols (e.g. sulphate and nitrate) are often mixed with natural aerosols (e.g. mineral dusts and sea salts). Subsequently, the complex mixture is transported over Japan en route to the north Pacific (Uematsu et al., 2002). Aerosols that are transported through the FT might travel intercontinental

*Corresponding author.
e-mail: kosada@nagoya-u.jp
DOI: 10.1111/j.1600-0889.2007.00296.x

distances from East Asia to North America (Jaffe et al., 2003). For that reason, the free troposphere over Japan is an important pathway of long-range transportation of materials from the Asian mainland to the Pacific Ocean in the atmosphere. However, knowledge of physical and chemical properties of aerosol particles in the FT near Japan, at the western entrance of the north Pacific, is limited to short-term snapshots based on observations made from aircraft (Dibb et al., 1996, 1997, 2003; Mori et al., 1999; Kline et al., 2004; Inomata et al., 2006) or on mountains (see below).

For physical data of aerosols in the FT over central Japan, seasonal variation of number-size distribution was reported at Mt. Tateyama based on continuous interannual measurements using an optical particle counter (Osada et al., 2003). That study showed differences of seasonal variations of coarse (spring maximum) and fine (early summer maximum) aerosol concentrations. It was further suggested that seasonal variations are related to changes in the dominant air trajectory and transport duration from major source areas, where huge amounts of SO_2 are emitted. Measurements of number-size distribution using an optical particle counter can elucidate the physical aspects of aerosols, but they cannot elucidate the chemical aspects of aerosols. At ground level, several studies have been made of the year-round seasonal variation of aerosol constituents in Japan [e.g. Mukai et al. (1990) at Oki Is., and Ohta and Okita (1990) at Sapporo]. However, year-round characterization of the FT aerosol chemistry over Japan and East Asia has never been reported. Because our previous chemical data of the FT aerosols were obtained for a selected period from winter to spring at Mt. Tateyama (Kido et al., 2001a,b) and late summer to fall at Mt. Norikura (Osada et al., 2002), adding further data from spring to fall might elucidate the seasonal variation of the aerosol chemistry over Japan.

We performed aerosol and other atmospheric observations at Mt. Norikura (36.1°N, 137.5°E), central Japan from mid-May to mid-October in 2001 and 2002 to fill the data gap from spring to fall. First, we present temporal variation of ionic concentrations during warm seasons. After defining the cases of low and high concentration samples, major factors controlling ionic concentrations in FT aerosols will be discussed with backward air trajectories regarding mixing with lower atmosphere and precipitation scavenging. Finally, combined with our previous data, this study will examine factors relating to seasonal variation of ionic species in FT aerosols over Japan.

2. Field and laboratory experiments

Atmospheric observations were performed at the Norikura Cosmic-ray Observatory (2770 m a.s.l.), Institute for Cosmic Ray Research, University of Tokyo, near the top of Mt. Norikura, central Japan during 15 May–15 October 2001 and during 15 May–15 October 2002. Figure 1 depicts a map with locations of Mts. Norikura (3026 m) and Tateyama (3015 m). No large urban or industrial areas exist near the mountains. Local cities, Takayama and Matsumoto, are located, respectively, at about 30–40 km west and east of Mt. Norikura. Mt. Tateyama is located about 50 km north of Mt. Norikura. Local cities, Toyama and Nagano, are located, respectively, at about 40–50 km west–northwest and east of Mt. Tateyama.

To check atmospheric conditions suitable for FT air sampling, ozone and number-size distribution of aerosol particles were measured using a Dasibi-type UV absorption O_3 monitor (1150;

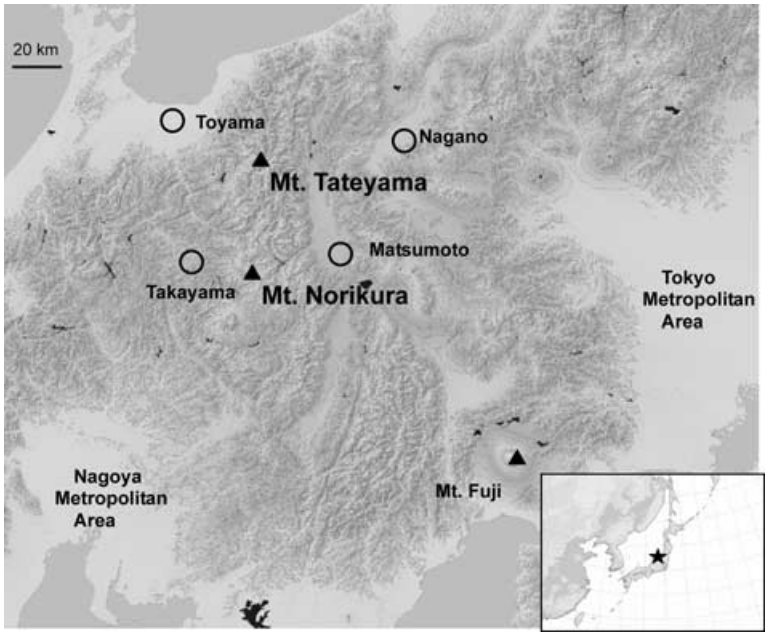

Fig. 1. Map of Mts. Norikura and Tateyama, central Japan. Cities are indicated as circles.

Tokyo Dylec Corp.) and an optical particle counter (KC-01D; Rion Co. Ltd.), respectively (Osada et al., 2002). Meteorological parameters were recorded using a data logger (Mini-met 3; Grant Instruments) and were logged on a memory board.

Inherent obstacles to atmospheric observations at high-elevation sites are upslope valley winds and downslope mountain winds (Mendonca, 1969; Nyeki et al., 1998; Seibert et al., 1998); they occur often on the slopes of Mts. Norikura and Tateyama. The upslope valley winds are caused by surface heating of the mountain slope by solar radiation during the daytime. The downslope mountain winds are caused by radiative cooling of the mountain surface during nighttime (Whiteman, 2000). Dense cooler air flows down the mountain slope, flushing the mountain surface with the FT's clean air. Daily variations of atmospheric parameters are examined as follows to determine the best condition to sample FT air at the site in Mt. Norikura.

Figure 2 shows variations of (a) O_3 concentrations and hourly precipitation, (b) number concentration of aerosols with particles of diameters larger than 0.3 and 1.0 μm and (c) averaged diurnal ratios for O_3 and aerosols during non-precipitation periods. To avoid local scavenging effects of precipitation, data of seven non-precipitation d (26 September–1 October and 3–5 October, 1999), as indicated by horizontal arrows in the lower part of the Fig. 2a, are included for calculating averaged diurnal variation ratios; then the hourly ratios to daily averages were combined for those 7 d. The O_3 and aerosol concentrations showed clear diurnal variations inversely: high in nighttime and low in daytime for O_3, low in nighttime and high in daytime for aerosols. Similar diurnal variation was found for Mt. Tateyama (Osada et al., 2003). Higher concentrations of aerosols during daytime are associated with vertical upward transportation of pollutants from lowland areas near the mountain. Lower concentrations of aerosols during nighttime (2200–0600) are attributed to the subsidence of clean air from FT aloft. Similarly, high and stable O_3 nighttime concentrations result from the subsidence of the O_3-rich air from the FT. Consequently, to collect the FT aerosols, our automated sampler was time-controlled and set to operate every morning (2400–0600).

The automated aerosol sampler was developed in-house to achieve unmanned long-term nighttime sampling at remote mountain sites. The Norwegian Institute for Air Research (NILU) filter holders were used to collect aerosol particles and were placed in a plastic weather shield having an open window at the bottom. Aerosol particles were collected using a Teflon membrane filter (pore size: 1.0 μm, filter size: 47 mm both in diameter; Advantec Toyo Kaisha Ltd.) at a flow rate of ca. 11 l min^{-1}. The sample air flow rate was measured using a mass flow meter (SEF-51; STEC Co. Ltd.) that was calibrated for standard temperature and pressure conditions. Concentrations of chemical constituents reported in this study are expressed under conditions of 0 °C and 1013 hPa.

During intensive observation periods, typically several days to 10 d during July–October, we also collected samples separately

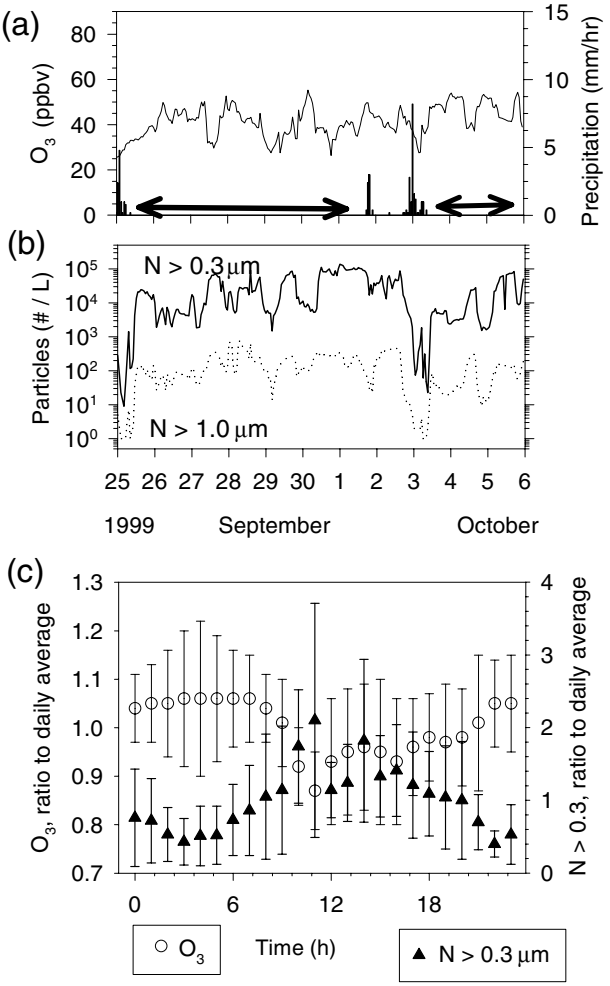

Fig. 2. Variations of (a) O_3 concentrations (ppbv) and hourly precipitation (vertical bars, mm h^{-1}), (b) number concentrations (l^{-1}) of aerosols larger than 0.3 and 1.0 μm diameter and (c) averaged diurnal variation ratios for O_3 and aerosols. In (c), ratios to the daily average are averaged for the non-precipitation period (horizontal arrows in Fig. 2a: 26 September to 1 October and 3–5 October in 1999). The position of date labels at the bottom of (a) and (b) indicates midnight.

for atmospheric NH_3 measurements using two acid-impregnated filters (0.01 M oxalic acid in a 16/84 glycerol/methanol solutionby volume) following the PTFE membrane filter. The NH_3 sampling was conducted during nighttime to synchronize the automated aerosol sampling during the intensive observation periods for 3 yr from 2000.

After sampling, each aerosol filter sample was put into a precleaned polypropylene 15 ml centrifuge vial with an airtight cap (Iwaki Glass Co. Ltd.). These vials were sealed in plastic bags to prevent contamination from ambient gases and were kept frozen until chemical analyzes at our laboratory. We obtained several procedural blank samples during the observation to evaluate possible contamination through sample handling and

storage. Procedural blank samples were treated identically to actual aerosol samples. Concentrations of procedural blanks were mostly negligible but, when present, they were subtracted from the values in the actual sample. To extract water-soluble components in the aerosol particles, we added 14 ml of ultrapure water (Milli-Q; Millipore Corp.) to the sample vial and immersed it for about 24 h. We applied neither ultrasonic treatment (increasing NO_2^- and NO_3^- concentration) nor ethanol wetting (which cannot measure trace amounts of weak acids and Cl^-) for extraction. Although the extraction efficiency of water soluble components from a PTFE filter might be time-dependent (Derrick and Moyers, 1981), immersion longer than 24 h and hand shaking was sufficient to extract nearly 100%. Ionic constituents and pH of water extracts of the filtered sample were analyzed using an ion chromatograph (IC: DX-300; Dionex Corp.) and a pH meter (Φ34, Beckman Coulter Inc.). Using typical sample air (3.5 m^3) and extracted water volume (14 ml), detection limits of aerosol constituents were estimated as about 20 ng m^{-3} for major ions (NO_3^-, SO_4^{2-}, Na^+, NH_4^+, K^+ and Ca^{2+}) and about 4 ng m^{-3} for oxalate. Details of the chemical analyzes were reported in Kido et al. (2001a) and Osada et al. (2002). Non-sea-salt (nss) concentrations of SO_4^{2-}, Ca^{2+} and K^+ were estimated from Na^+ contents in the sample according to their respective ratios in seawater (Wilson, 1975).

Data of aerosol and NH_3 concentrations used here are selected for samples without precipitation to avoid local effects of aerosol-scavenging by rain. Another limitation of data selection is the local wind direction during sampling. Volcanic emissions of SO_2 and ash from Mt. Asamayama, located about 90 km ENE of the site, increased in 2002. Data of aerosol samples collected during periods of easterly winds are excluded from this study to avoid volcanic effects and local contamination. For this study, 233 samples were obtained during the two warm periods of 2001 and 2002. Among them, 142 samples were of non-precipitating conditions and 104 samples were of both non-precipitating and non-easterly wind conditions.

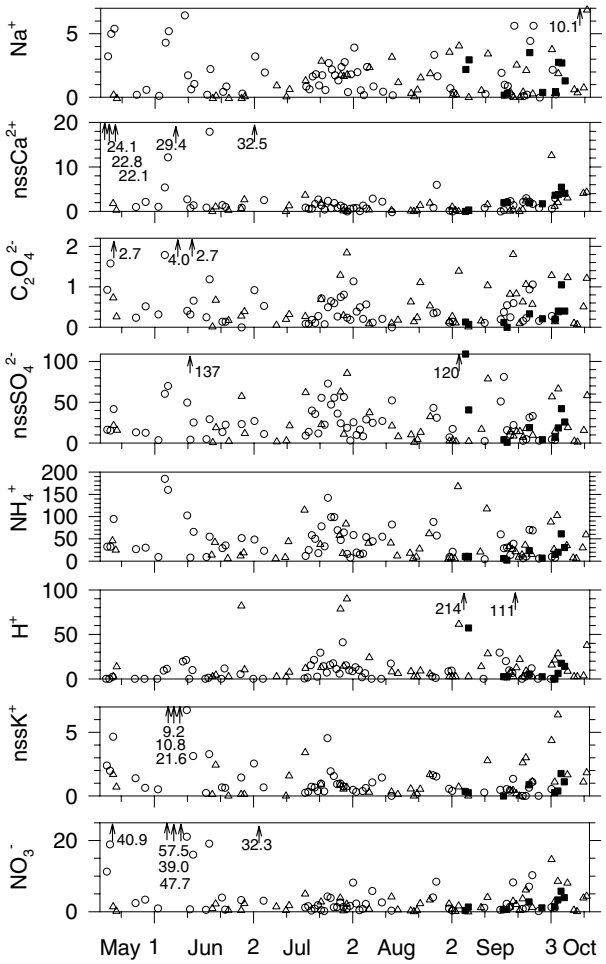

Fig. 3. Temporal variations of ionic concentrations (nmol m^{-3}) of aerosols as composite plots for 2001, open circles, and 2002, triangles. Data (1 September–8 October 2000) of the previous report (filled squares) are also included (Osada et al., 2002).

3. Results and discussion

3.1. Short-term variation and co-varying ions in the warm season

Figure 3 shows variations of ionic concentrations of FT aerosols as composite plots for 2 yr. Data (10 samples for 1 September–8 October 2000) of the previous report (Osada et al., 2002) are also included. Sporadically high concentrations for all ions shown are observed in May–June, especially for $nssCa^{2+}$, $C_2O_4^{2-}$, $nssK^+$ and NO_3^-. For $nssCa^{2+}$ and NO_3^-, they are apparently low concentrations in July–mid-September. Concentrations of Na^+, $nssK^+$ and $C_2O_4^{2-}$ are lower and less variable in August. The dominant ionic species in the aerosols are $nssSO_4^{2-}$ and NH_4^+. As fractions of total ionic weights of aerosols, $nssSO_4^{2-}$ and NH_4^+, respectively account for ca. 60% and *ca.* 20% on average, except for samples with high H^+ and $nssCa^{2+}$ contents. The average, median, *SD*, and the minimum and maximum concentrations of the total ionic weight of the 114 samples in Fig. 3 were, respectively, 3.9, 2.8, 3.7, 0.2 and 23.2 $\mu g\ m^{-3}$. Based on the range of temporal variation and variability in Fig. 3, we can classify the data at Mt. Norikura into three periods: May–June (MJ), July–August (JA), and September–October (SO). We will use this classification later in Section 3.4.

Expanded temporal variations between 1 June and 2 July 2001 are shown in Fig. 4 to illustrate day-to-day variation and relationship among ions. This period includes maximum concentrations of $nssSO_4^{2-}$, NH_4^+, $C_2O_4^{2-}$, NO_3^- and $nssCa^{2+}$ in Fig. 3. As described in Section 2, data plotted here were selected according to their local meteorological conditions: dry, with non-easterly winds. At the top of Fig. 4, the duration of the easterly wind is indicated at 'E' with bold underlining. Together with this, rain intensity and relative humidity in the top panel describe the

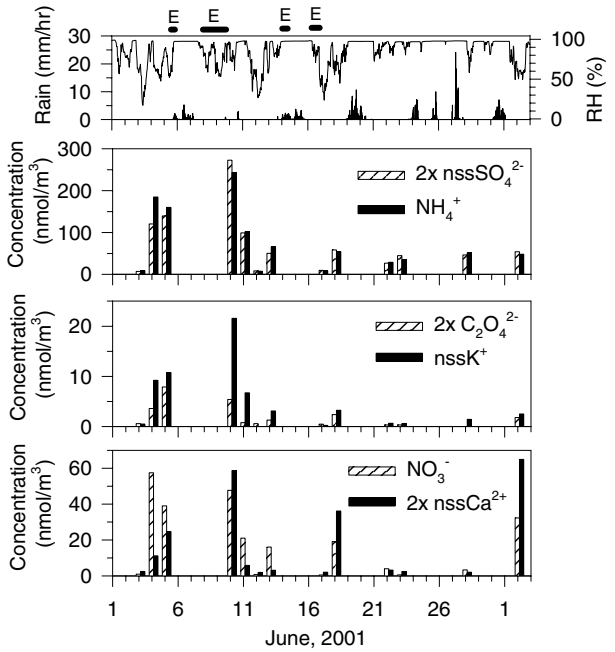

Fig. 4. Short-term variations of ionic concentrations between 1 June and 2 July 2001. Vertical lines and line plot in the top panel, respectively represent the precipitation amount and relative humidity. Duration of the easterly wind is indicated as E at the top.

situation of meteorological conditions for aerosol sampling. Although the unit of concentration in Fig. 4 is nmol m^{-3}, the concentration of divalent ions is doubled for ionic balance comparison purposes.

Concentrations of $nssSO_4^{2-}$ are correlated well with NH_4^+, implying the existence of ammonium sulphate for the samples in this period. Temporal variation of $nssK^+$ and $C_2O_4^{2-}$ concentrations are also mostly in phase and tend to synchronize with variations of $nssSO_4^{2-}$ and NH_4^+. Part of temporal variation of NO_3^- concentration co-vary with NH_4^+, but also tend to exhibit similar 'high' and 'low' episodes with $nssCa^{2+}$, except for June 4 of a high NO_3^- event. Because Kosa particles containing $CaCO_3$ act as aeolian carriers of NO_3^- (Nishikawa et al., 1991; Ooki and Uematsu, 2005), $nssCa^{2+}$ and NO_3^- might be transported together after chemical transformation. Among these ions, stoichiometric correlation is apparent only for $nssSO_4^{2-}$ and NH_4^+.

Figure 5 shows scatter plots of $nssSO_4^{2-}$ and NH_4^+ or NH_4^+ plus H^+ concentrations. Most samples with less than 30 nmol m^{-3} of $nssSO_4^{2-}$ are plotted on the 1:2 line with NH_4^+ alone, implying that most of $nssSO_4^{2-}$ exists as ammonium sulphate, fully neutralized by NH_4^+. On the other hand, for samples with greater than 30 nmol m^{-3}, $nssSO_4^{2-}$ concentrations are distributed below the 1:2 line. Considered together with H^+ concentrations (lower panel), most $nssSO_4^{2-}$ plus H^+ concentrations are balanced with NH_4^+.

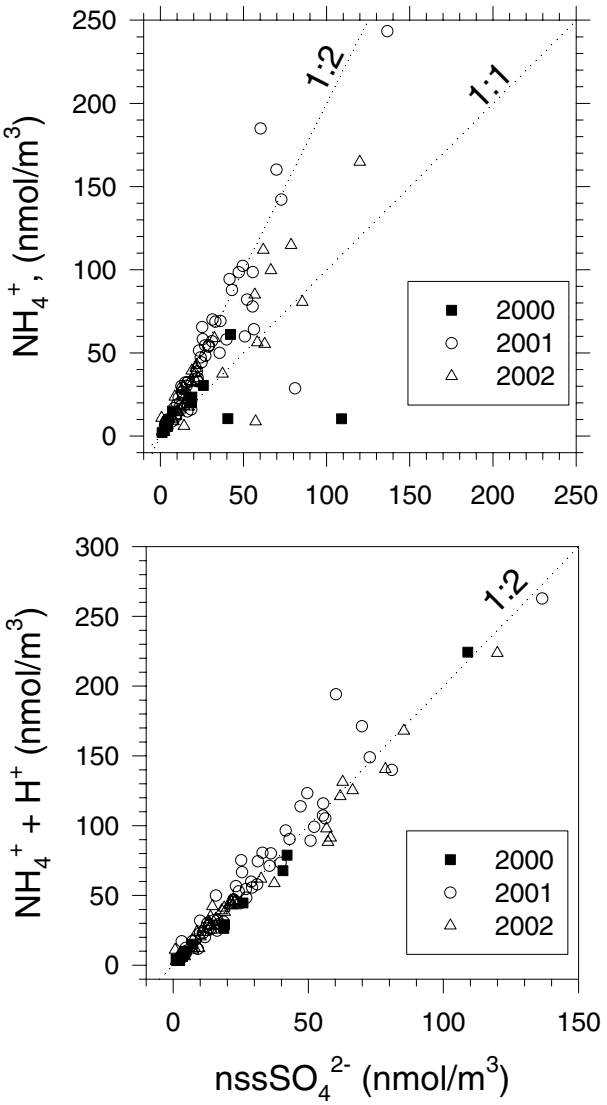

Fig. 5. Relationship between $nssSO_4^{2-}$ and NH_4^+ or $NH_4^+ + H^+$ concentrations.

3.2. *Transport condition of aerosols for low and high concentration cases*

In this section, we explain factors that control the low and high ionic concentrations observed in Fig. 3. Horizontal and vertical transport conditions are examined for low- or high-concentration cases based on backward air trajectory (HYSPLIT 4; Draxler and Rolph, 2003) with precipitation amount along the route (Seibert et al., 1998; Nishita et al., 2007). The starting height and time of the trajectories were set, respectively as 3000 m a.s.l. at Mt. Norikura and the mid-point of the sampling period (03 LT). Using total ionic concentration, 25 samples with less than 1 μg m^{-3} were selected for low concentration cases. The value of the total ionic weight of aerosols corresponds to *ca.* 7.5 nmol m^{-3} of $nssSO_4^{2-}$, assuming that all aerosols consist of $(NH_4)_2SO_4$.

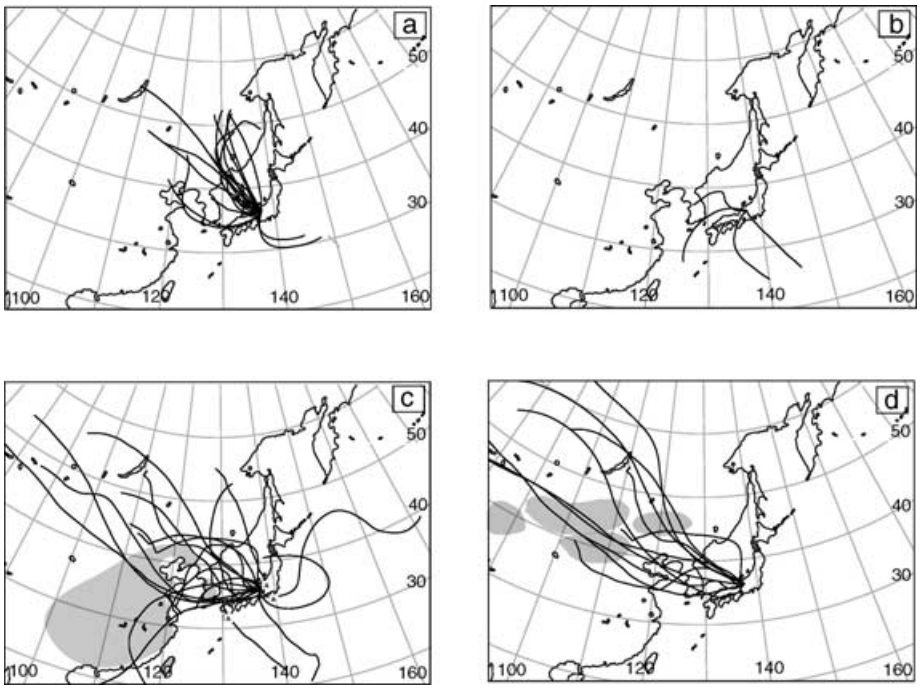

Fig. 6. Horizontal plots of backward air trajectories: (a) cases for total ionic concentration below 1 μg m^{-3} with cumulative rain less than 5 mm during the preceding 2 d, (b) Same as *a* but for more than 5 mm rain, (c) high nssSO_4^{2-} (>50 nmol m^{-3}) and (d) high nssCa^{2+} (>5 nmol m^{-3}). Hatched areas and filled triangles in *c* represent major source regions of SO_2 and active volcanoes. Hatched areas in (d) indicate emission source areas of Asian dusts.

For high concentration cases, 20 and 11 samples were selected, respectively as high nssSO_4^{2-}(>50 nmol m^{-3}) and high nssCa^{2+} (>5 nmol m^{-3}). In these samples, SO_4^{2-} alone comprises about 60% of total ionic weight, on average. Therefore, selecting high-SO_4^{2-} samples implies selection of higher total ionic concentrations, except for samples with high-Ca content influenced by Kosa dusts. As depicted in Fig. 4, high nssCa^{2+} on July 2 did not accompany high nssSO_4^{2-}, suggesting that a different factor exists to enhance Ca-rich aerosols. For that reason, cases of high Ca^{2+} concentration were considered separately, as described below.

Figure 6 shows horizontal plots of backward trajectories: *a* (21 samples) and b (four samples) for low concentration cases with cumulative rain of less and more than 5 mm during the preceding 2 d, and c and d, respectively, for high concentration cases of nssSO_4^{2-} and nssCa^{2+}. The durations of backward trajectories in Figs. 6c and d are 5 d instead of the 2 d for Figs. 6a and b. Major source areas of Kosa dust (Fig. 6d) for nssCa^{2+} and anthropogenic pollutants (Fig. 6c) for nssSO_4^{2-} are indicated as hatched areas (Pye, 1987; Sun et al., 2001; Kanayama et al., 2002; Streets et al., 2003). Locations of major active volcanoes in Japan are also marked by triangles: Asamayama, and Miyakejima and Sakurajima islands (Fujita et al., 2003; Current Eruptions in Japan, http://hakone.eri.u-tokyo.ac.jp/vrc/erup/erup.html). Figure 7 shows vertical plots of backward trajectories with hourly precipitation amounts along the route. Panels a to d in Fig. 7 correspond to the same categories as those for Fig. 6.

No matter where air parcels travelled, precipitation scavenging immediately before arrival might have strongly reduced the aerosol mass concentration, especially for air parcels that were exposed to in-cloud scavenging (see the review in Warneck, 1999). For that reason, we carefully avoided data that were influenced by local rain and fog events at the site. For low concentration samples (Figs. 6a and b), horizontal trajectories during the prior 2 d spread around Japan from the southeast clockwise to the north direction, mostly within 2000 km from the site. Note that trajectory routes and endpoints tend to locate over the ocean or over less-industrial regions. During 2 d, most trajectories descended from higher altitudes (4–6 km) to the site (Fig. 7a), except for ascended or waved cases, which were influenced by precipitation scavenging (Fig. 7b). Although the vertical profile of aerosol mass concentration might not simply decrease with increasing altitude (Kline et al., 2004), it is generally considered as lower in the FT (Jaenicke, 1993; Sakai et al., 2000). For that reason, air that has descended from a higher altitude might display a lower mass concentration. Detailed analyzes of three-dimensional trajectories suggest that low concentration samples were obtained at the site when the position descended to 3 km (altitude of the site) is over the sea or a less polluted area. Although the thickness of atmospheric boundary layer is variable

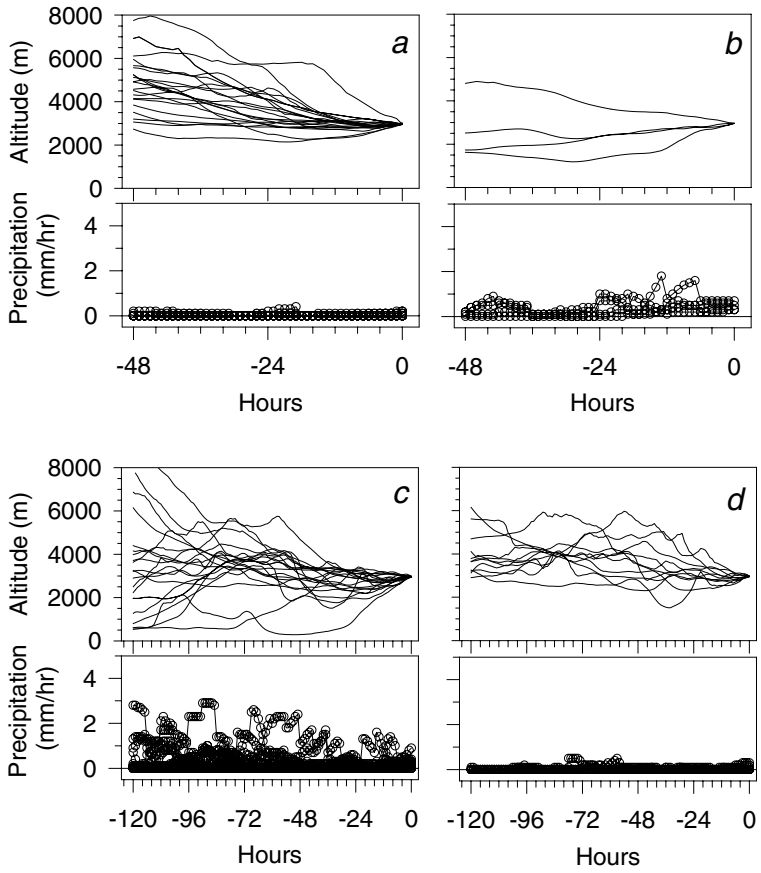

Fig. 7. Vertical plots of backward trajectories (upper) and hourly precipitation amounts (lower) along the trajectory. Cases plotted for a–d are as indicated in Fig. 6.

with respect to location and time, typically several hundred meters to several kilometres (Stull, 2000), it might be thinner over the sea than over the continent because of lower surface heating by solar radiation. This difference of layer thickness engenders a reduced probability of entraining aerosols that are rich in the continental boundary layer.

Trajectories showing ascension or waved cases in Fig. 7*b* experienced precipitation of more than 5 mm during the preceding 2 d. Although the amount of cumulative rain is not large, low aerosol concentrations might result from precipitation scavenging within a short duration. The trajectories of Fig. 6b were located mostly over the sea and rarely contacted with polluted boundary layer; consequently, they displayed a low aerosol concentration after precipitation scavenging.

Examination of trajectories in Fig. 6c suggests that high $nssSO_4^{2-}$ concentrations might be attributed to contact of air parcels with strong anthropogenic emission areas and volcanic plumes. Although some trajectories accompanied precipitation during 5 d (Fig. 7c), entrainment of pollution or volcanic plumes after precipitation scavenging might engender high aerosol contents in the arriving air. Volcanic influences on high $nssSO_4^{2-}$ concentrations are often apparent during summer because huge amounts of SO_2 were emitted from Miyakejima Island during and after August 2000 (Fujita et al., 2003; Satsumabayashi et al., 2004).

Almost no precipitation was estimated for trajectories of high $nssCa^{2+}$ cases in Fig. 7d, but vertical trajectories showed undulation. Horizontal positions of trajectories passed over desert and loess areas (Fig. 6d). Because the trajectories passed over dusty regions and because the air revealed high Ca contents of aerosols (Ichikuni, 1978; Suzuki and Tsunogai, 1988), it is inferred that the aerosol samples contain Kosa dust.

To summarize the information given in this section, factors that lead to low aerosol mass concentration at the site are descending trajectories and precipitation scavenging during transport without contact with the boundary layer atmosphere until arrival. Factors to enhance mass concentration in the FT aerosols are the connection with active emissions at the surface without precipitation scavenging after entrainment.

3.3. Correlation of FT aerosols between Mts. Norikura and Tateyama

We have taken measurements at Mt. Tateyama for the winter–spring period (Kido et al., 2001a,b). To obtain a year-round data set for the FT aerosol chemistry over Japan, uniformity

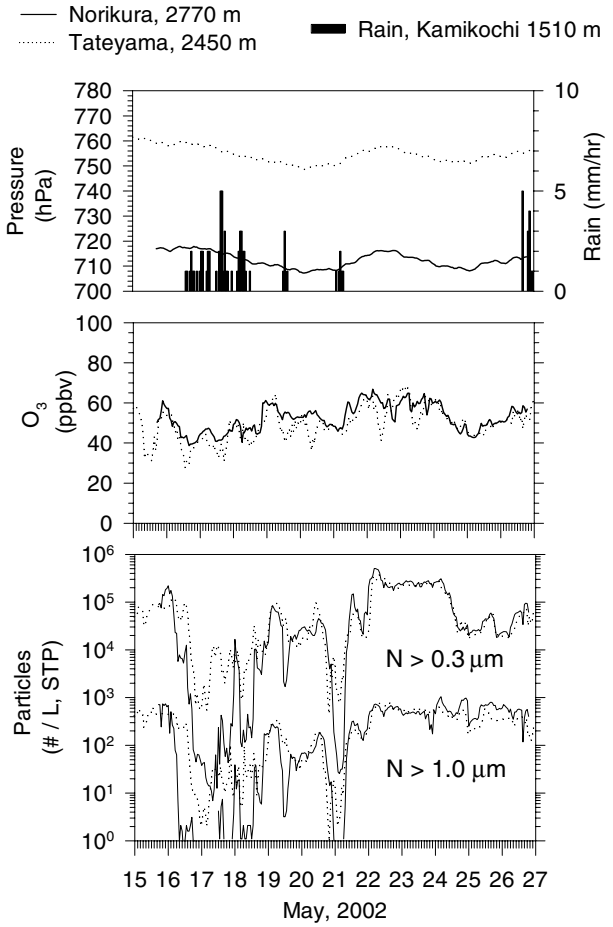

Fig. 8. Comparison of atmospheric pressure, hourly precipitation at Kamikochi (intermediate of both sites), O_3 and aerosol concentrations ($N > 0.3$ and 1.0 μm) at Mts. Norikura (thin line) and Tateyama (dotted line).

of aerosol concentration and synchroneity of temporal variation at the height range of mountains were examined using continuous data taken from Mts. Norikura and Tateyama. Figure 8 shows an example of time variations at the sites for atmospheric pressure, O_3 and aerosol concentrations ($N > 0.3$ and 1.0 μm). Hourly precipitation at Kamikochi (at about the midpoint between both sites) is also plotted in Fig. 8 to show the duration of aerosol scavenging by regional scale precipitation. Although Mt. Tateyama is located about 50 km north, general trends of atmospheric pressure, O_3, and aerosols show similar variations. The number concentrations of aerosols during rainy days, as on May 16–19 and May 21, are different between the sites, probably because of precipitation scavenging. In contrast, nighttime data during non-precipitation periods agree well, suggesting that aerosol concentration at the altitude of the sites is laterally uniform in this area under the non-precipitating FT condition. Therefore, selecting non-precipitating nighttime conditions for both sites might provide year-round data that are complementary to those observed during different seasons. Assuming that non-precipitating nighttime data represent uniformly distributed FT aerosol chemistry over central Japan, we next combine the data from Mt. Tateyama to examine year-round chemical aspects of FT aerosols over Japan.

3.4. Year-round variation of aerosol chemistry over central Japan

Figure 9 shows box plots of ionic concentrations of aerosols at Mts. Norikura (May–October, this study) and Tateyama (November–April, Kido et al., 2001a,b). As described in Section 3.1, data of Mt. Norikura are classified into three periods: MJ, JA and SO. Data from Mt. Tateyama are classified into two seasons: winter (NDJF: November–February) and spring (MA: March and April). Table 1 lists averages and medians of those data. As shown in Fig. 9 and Table 1, most average values are higher than their median, reflecting that several high outlier values exist in the dataset.

Most average concentrations are high in spring and MJ, with large variation. Except for Na^+, they are low in winter. Winter minima of various constituents in FT aerosols have also been reported for Mauna Loa (Hawaii, central Pacific; Lee et al., 1994; Perry et al., 1999; Huebert et al., 2001), Sonnblick Observatory (eastern European Alps; Kasper and Puxbaum, 1998), Jungfraujoch (central European Alps; Henning et al., 2003), and Vallot Observatory (western European Alps; Preunket et al., 2002).

The Na^+ concentration is high in spring, but it is almost constant for other seasons. Average concentrations of NO_3^-, $nssCa^{2+}$, $nssK^+$ and $C_2O_4^{2-}$ in summer are almost equal to those in fall: values are intermediate between spring high and winter low values. Except for $nssCa^{2+}$, these species are considered to originate mainly from anthropogenic combustion sources or biomass burning (Andreae, 1983; Kawamura and Kaplan, 1987; Narukawa et al., 1999). Although a natural production mechanism through cloud processing has been proposed for $C_2O_4^{2-}$ in a clean atmosphere (Warneck, 2003, 2005; Ervens et al., 2004), its correlation with other anthropogenic species in short-term and seasonal variations suggests that contribution of natural production might not be large to modify $C_2O_4^{2-}$ levels in FT aerosols over Japan.

For $nssCa^{2+}$ concentration, its seasonal variation might depend on the outbreak frequency of dust storms in continental Asia's desert areas, which is low in winter and summer, and high in spring (Kurosaki and Mikami, 2003). In addition, seasonal change of major transport pathways inhibits Kosa dust transportation from the west (Fig. 6d) because transport of Pacific air is more common in summer (Osada et al., 2003).

The maximum of the average $nssSO_4^{2-}$ concentration occurs in summer with continuously high concentrations from spring to fall. As discussed in Section 3.2, a major precursor of $nssSO_4^{2-}$ in the FT aerosols over Japan is inferred to be anthropogenic SO_2 from East Asia and volcanic SO_2 near Japan, with a very low contribution of marine DMS emission, as inferred from the

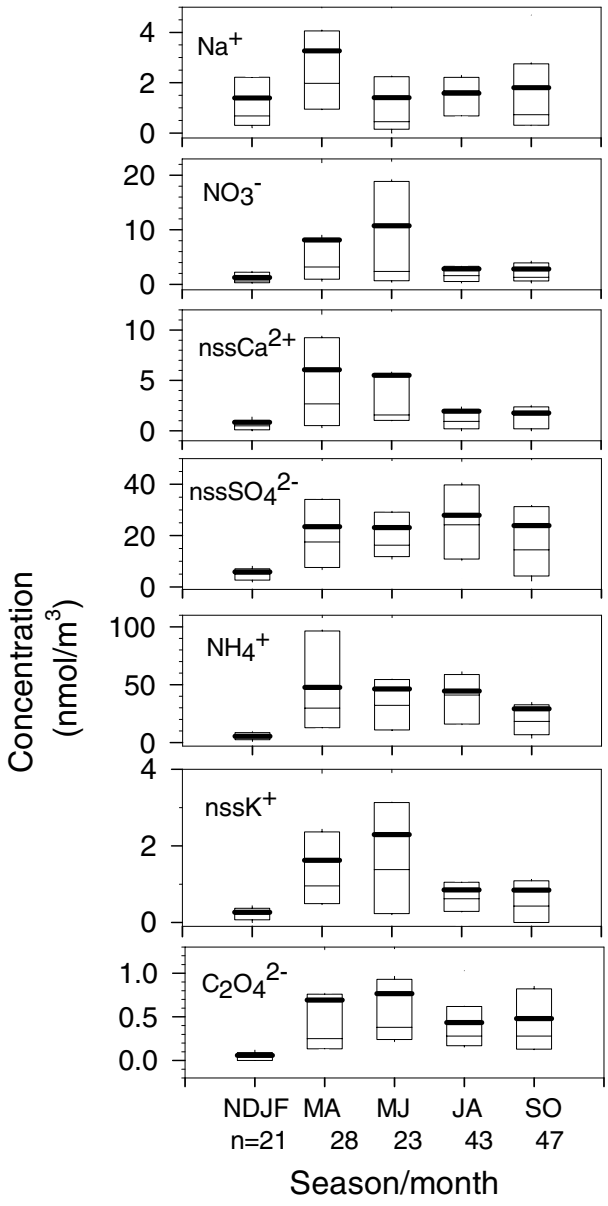

Fig. 9. Box plots of ionic concentrations (nmol m^{-3}) of aerosols at Mts. Norikura (May–October, this study) and Tateyama (November–April, Kido et al., 2001a,b). The boundary of the box closest to zero indicates the 25th percentile, thin and heavy lines within the box, respectively, represent the median and average. The boundary of the box located most distally from zero indicates the 75th percentile. MJ: May–June, JA: July–August, and SO: September–October, NDJF: November–February, and MA: March–April. Numbers (n =) represent the number of data used.

molar ratio (*ca.* 0.2% on average for 2001) of $CH_3SO_3^-/nssSO_4^{2-}$ (not shown). Seasonal variation of SO_2 emissions in East Asia increases slightly in winter (Streets et al., 2003). However, seasonal variation of $nssSO_4^{2-}$ that is observed over Japan differs from that of SO_2 emission in East Asia. According to measurements taken at Mt. Fuji (Igarashi et al., 2004, 2006), the SO_2 concentration was high, with many episodic peaks larger than 1 ppbv in winter, and low with fewer spikes in summer. Considering seasonal variations of SO_2 concentration at Mt. Fuji and our $nssSO_4^{2-}$ in aerosols together, the ratio of sulphate aerosols to total sulphur in molar units, $SO_4^{2-}/(SO_4^{2-} + SO_2)$, is expected to be high in summer and low in winter. The winter minimum of $nssSO_4^{2-}$concentration in aerosols might be ascribed to (1) the lower rate of SO_2 oxidation during colder and darker winters (Warneck, 1999) and (2) faster transport from SO_2 source areas to Japan (Kido et al., 2001a; Inomata et al., 2006). Alternatively, opposite conditions of oxidation and transport processes might engender efficient formation of $nssSO_4^{2-}$ in aerosols in warm months (Osada et al., 2003). In addition, frequency of volcanic influences tends to increase in summer, as shown in Fig. 6c.

Seasonal variation of average NH_4^+ concentrations shows high values during spring and summer, decreasing gradually in fall to the winter minimum. Major sources of ammonia include combustion, bacterial decomposition of animal excreta, and emission from soil and vegetation (Warneck, 1999). Among them, emanation from fertilizer application and animals are considered to be main sources in East Asia (Streets et al., 2003). According to estimates by Streets et al., NH_3 emissions in China vary according to the season: they are high during March–July and low during October–February, mainly because of fertilizer usage and temperature effects of emanation from agricultural soils (Fig. 10a). Different from SO_2 emissions in China, the maximum/minimum ratio of NH_3 seasonal variation is about 2. Figure 10b shows total NH_x ($NH_3 + NH_4^+$) and NH_3 concentrations of FT aerosols at Japan. Although NH_3 data for the MJ season are unavailable, seasonal variations of NH_x and NH_3 concentrations show a spring maximum and winter minimum. The maximum/minimum ratio (*ca.* 8) of NH_x concentration is much greater than that of NH_3 emissions in China. Values of average particle fractions $NH_4^+/(NH_3 + NH_4^+)$ were from 68% in winter to 87% in JA and SO season, implying that more than half of NH_x exists as aerosol particles at sites, with small variation according to the season.

Seasonal variation of the molar ratio, $NH_4^+/nssSO_4^{2-}$ in aerosols is high (*ca.* 2) in spring and decreases to 1 in winter (Fig. 10c), implying a change of major chemical forms of sulphate from ammonium sulphate in spring to ammonium bisulphate in winter. According to aerial observation results, the molar ratios of aerosol $NH_4^+/nssSO_4^{2-}$ in the lower troposphere over the East China Sea and Bohai Sea were approximately 2 (Hatakeyama et al., 2004, 2005), suggesting rapid neutralization of acidic sulphates by ammonia, which is abundant in the spring atmosphere over China. Combined with transport processes considered in Section 3.2 and Hatakeyama's results, the existence of $(NH_4)_2SO_4$ over Japan in spring is ascribed to transport of fully neutralized sulphate at the major source area. For other seasons, aerial data over China are not available, thereby preventing our direct comparison of the molar ratio of aerosols with source

Table 1. Ionic concentrations of atmospheric aerosol particles (nmol m^{-3})

Location, altitude m a.s.l. Ref Period [number of samples, *n*]		(1) Na^+	(2) NO_3^-	(3) $nssSO_4^{2-}$	(4) NH_4^+	(5) $nssK^+$	(6) $C_2O_4^{2-}$	(7) $nssCa^{2+}$
Mt. Norikura, 2770 m	This study							
May–June [$n = 23$]		1.4	10.7	23.1	46.3	2.3	0.8	5.5
		(0.5)	(2.4)	(16.3)	(32.2)	(1.4)	(0.4)	(1.6)
July–August [$n = 43$]		1.6	2.8	28.0	44.5	0.9	0.4	1.9
		(1.7)	(1.6)	(14.5)	(41.0)	(0.6)	(0.3)	(0.9)
September–October [$n = 47$]		1.8	2.8	23.9	29.1	0.8	0.5	1.8
		(0.7)	(1.3)	(16.2)	(18.3)	(0.4)	(0.3)	(1.6)
Mt. Tateyama, 2450 m								
Winter, 1995–2000 [$n = 21$]	a	1.4	1.3	5.9	5.5	0.3	0.1	0.8
(November–February)		(0.7)	(0.6)	(5.0)	(4.5)	(0.2)	(0.1)	(0.5)
Spring, 1996–2000 [$n = 28$]	b	3.3	8.2	23.5	47.7	1.6	0.7	6.1
(March–April)		(2.0)	(3.2)	(17.5)	(29.8)	(1.0)	(0.3)	(2.7)

Data in parentheses are median values.
Values below the detection limit were set to 50% of the detection limit for each ion.
References: a, Kido et al. (2001a) and b, Kido et al. (2001b).

areas. However, estimates of the source intensity for NH_3 and SO_2 (Streets et al., 2003) might facilitate the interpretation of seasonal variation of the molar ratio. Although the seasonal variation of SO_2 emission in China is nearly constant throughout the year, NH_3 emissions are high during March–July. For that reason, the molar ratio of NH_3 to SO_2 in gas phase at the source area might follow the seasonal variation of NH_3 emission (Fig. 10a). Annual emission rates of SO_2 and NH_3 in China were estimated as 0.3 and 0.8 Tmol yr^{-1}, indicating that more NH_3 was emitted over SO_2 to form $(NH_4)_2SO_4$ annually, but in fall to winter, emission of NH_3 lacked to fully neutralize SO_4^{2-} oxidized from SO_2. The lower values of the gaseous molar ratio from fall through winter agree with observations of FT aerosols over Japan. As a consequence, the variation of gaseous molar ratio at the source area in China might lead to seasonal variation of the molar ratio in aerosols in the FT over Japan.

4. Summary and conclusions

Free tropospheric aerosols were collected using an automated aerosol sampler at Mt. Norikura, central Japan, from mid-May to mid-October in 2001 and 2002 to close the seasonal gaps in data sets for this area. Considered along with previously reported data (November–April, Kido et al., 2001a,b), this report is the first to describe year-round variation of the FT aerosol chemistry for East Asia. This paper has presented short-term and seasonal variations of ionic concentrations in relevance with controlling factors of their variations.

Based on analyzes of backward air trajectories with precipitation amounts along the route, characteristic transport conditions were discussed for low- and high-concentration samples. The analyzes suggest that factors engendering low aerosol mass concentrations are (1) trajectories in descending motion and (2) precipitation scavenging during transport without contacting the boundary layer atmosphere until arrival, and that the factor that enhances mass concentration is connection with active emissions at the surface without precipitation scavenging after entrainment.

Average concentrations of NO_3^-, $nssK^+$ and $C_2O_4^{2-}$ are high in March–June with large variability, and low in winter. The dominant ionic species in the FT aerosols are $nssSO_4^{2-}$ and NH_4^+ for all seasons. The maximum of average $nssSO_4^{2-}$ concentrations occurs in summer; those concentrations remain continuously high from spring through fall. The pattern of seasonal variation of NH_4^+ concentrations resembles that of $nssSO_4^{2-}$, but their molar ratio ($NH_4^+/nssSO_4^{2-}$) is high (*ca.* 2) in spring and decreases to 1 in winter, implying a change of major chemical forms of sulphate from ammonium sulphate in spring to ammonium bisulphate in winter. Considered along with NH_3 data at the site and emission data obtained by Streets et al. (2003) at the source area, the variation of gaseous molar ratio (NH_3/SO_2) in China might engender seasonal variation of the molar ratio in aerosols in the FT over Japan.

5. Acknowledgments

The authors thank the staff of the Norikura Cosmic Ray Observatory, ICRR, University of Tokyo for their warm hospitality and help with our work. We are grateful to Drs. Muraki and Matsubara, STEL, Nagoya University for encouraging this work at the observatory. The authors gratefully acknowledge the NOAA Air Resources Laboratory (ARL) for providing the HYSPLIT transport model website (http://www.arl.noaa.gov/ready.html) described in this publication. The authors are also grateful to

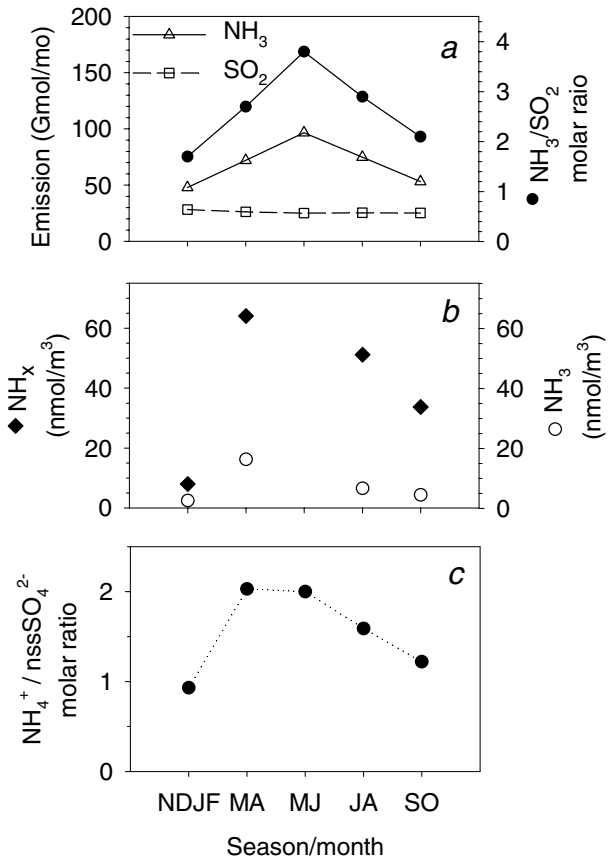

Fig. 10. Seasonal variation of (a) averaged monthly emission flux for the period (open triangle: NH_3, open squares: SO_2) and molar ratio (filled circles) in China, (b) NH_x (filled diamonds, $NH_4^+ + NH_3$) and NH_3 (open circles) concentrations at the mountain sites and (c) molar ratio in aerosols at the sites calculated from average values of the periods. Data of NH_x ($NH_4^+ + NH_3$) and NH_3 for MJ are not available.

Dr. D.G. Streets for providing data of monthly emission flux in China. This work was supported by the Ministry of Education, Culture, Sports, Science and Technology, a Grant-in-Aid for Scientific Research on Priority Areas (nos. 10144104, 10144211, 11131210, 12018207), and by Grants-in-Aid for Scientific Research (C) 13680601 and (B) 15310012 from the Ministry of Education, Culture, Sports, Science and Technology.

References

Andreae, M. O. 1983. Soot carbon and excess fine potassium: long-range transport of combustion-derived aerosols. *Science* **220**, 1148–1151.

Andreae, M. O. 1995. Climatic effects of changing atmospheric aerosol levels. In: *Future Climates of the World: A Modeling Perspective* World Survey of Climatology, Volume 16 (ed. A. Henderson-Sellers). Elsevier, Amsterdam, 347–398.

Charlson, R. J. and Heintzenberg, J. 1995. *Aerosol Forcing of Climate*. John Wiley, New York, pp. 416.

Derrick, M. and Moyers, J. 1981. Precise and sensitive water soluble ion extraction method for aerosol samples collected on polytetrafluoroethylene filters. *Anal. Lett.* **14**, 1637–1652.

Dibb, J. E., Talbot, R. W., Klemm, K. I., Gregory, G. L., Singh, H. B. and co-authors. 1996. Asian influence over the western North Pacific during the fall season: inferences from lead 210, soluble ionic species and ozone. *J. Geophys. Res.* **101**, 1779–1792.

Dibb, J. E., Talbot, R. W., Lefer, B. L., Scheuer, E., Gregory, G. L. and co-authors. 1997. Distributions of beryllium 7 and lead 210, and soluble aerosol-associated ionic species over the western Pacific: PEM West B, February–March 1994. *J. Geophys. Res.* **102**, 28287–28302.

Dibb, J. E., Talbot, R. W., Scheuer, E. M., Seid, G., Avery, M. A., and co-authors. 2003. Aerosol chemical composition in Asian continental outflow during the TRACE-P campaign: comparison with PEM-West B. *J. Geophys. Res.* **108**, doi:10.1029/2002JD003111.

Draxler, R. R. and Rolph, G. D. 2003. HYSPLIT (HYbrid Single-Particle Lagrangian Integrated Trajectory) Model access via NOAA ARL READY Website (http://www.arl.noaa.gov/ready/hysplit4.html). NOAA Air Resources Laboratory, Silver Spring, MD.

Duce, R. A., Unni, C. K., Ray, B. J., Prospero, J. M. and Merrill, J. T. 1980. Long-range atmospheric transport of soil dust from Asia to the tropical north pacific: temporal variability. *Science* **209**, 1522–1524.

Ervens, B., Feingold, G., Frost, G. J. and Kreidenweis, S. 2004. A modeling study of aqueous production of dicarboxylic acids: 1. Chemical pathways and speciated organic mass production. *J. Geophys. Res.* **109**, doi:10.1029/2003JD004387.

Fujita, S., Sakurai, T. and Matsuda, K. 2003. Wet and dry deposition of sulfur associated with the eruption of Miyakejima volcano, Japan. *J. Geophys. Res.* **108**, doi:10.1029/2002JD003064.

Hatakeyama, S., Takami, A., Sakamaki, F., Mukai, H., Sugimoto, N. and co-authors. 2004. Aerial measurement of air pollutants and aerosols during 20–21 March 2001 over the East China Sea. *J. Geophys. Res.* **109**, doi:10.1029/2003JD004271.

Hatakeyama, S., Takami, A., Wang, W. and Tang, D. 2005. Aerial observation of air pollutants and aerosols over Bo Hai, China. *Atmos. Environ.* **39**, 5893–5898.

Henning, S., Weingartner, E., Schwikowski, M., Gaggeler, H., Gehring, R. and co-authors. 2003. Seasonal variation of water-soluble ions of the aerosol at the high-alpine site Jungfraujoch (3580 m asl). *J. Geophys. Res.* **108**, doi:10.1029/2002/JD002439.

Husar, R. B., Prospero, J. M. and Stowe, L. L. 1997. Characterization of tropospheric aerosols over the oceans with the NOAA advanced very high resolution radiometer optical thickness operational product. *J. Geophys. Res.* **102**, 16889–16909.

Huebert, B. J., Phillips, C. A., Zhuang, L., Kjellström, E., Rodhe, H. and co-authors. 2001. Long-term measurements of free-tropospheric sulfate at Mauna Loa: comparison with global model simulations. *J. Geophys. Res.* **106**, 5479–5492.

Ichikuni, M., 1978. Calcite as a source of excess calcium in rainwater. *J. Geophys. Res.* **83**, 6249–6252.

Igarashi, Y., Sawa, Y., Yoshioka, K., Matsueda, H., Fujii, K. and co-authors. 2004. Monitoring the SO_2 concentration at the summit of Mt. Fuji and a comparison with other trace gases during winter. *J. Geophys. Res.* **109**, doi:10.1029/2003JD004428.

Igarashi, Y., Sawa, Y., Yoshioka, K., Takahashi, H., Matsueda, H., and co-authors. 2006. Seasonal variations in SO_2 plume transport over Japan: observations at the summit of Mt. Fuji from winter to summer. *Atmos. Environ.* **40**, 7018–7033.

Inomata, Y., Iwasaka, Y., Osada, K., Hayashi, M., Mori, I. and co-authors. 2006. Vertical distributions of particles and sulfur gases (volatile sulfur compounds and SO_2) over East Asia: comparison with two

aircraft-borne measurements under the Asian continental outflow in spring and winter. *Atmos. Environ.* **40**, 430–444.

Iwasaka, Y., Minoura, H. and Nagaya, K. 1983. The transport and special scale of Asian dust-storm clouds: a case study of the dust-storm event of April 1979. *Tellus* **35B**, 189–196.

Jaenicke, R. 1993. Tropospheric aerosols. In: *Aerosol-Cloud-Climate Interactions* (ed. P. V. Hobbs). Academic Press Inc., San Diego, 1–31.

Jaffe, D., McKendry, I., Anderson, T. and Price, H. 2003. Six 'new' episodes of trans-Pacific transport of air pollutants. *Atmos. Environ.* **37**, 391–404.

Kanayama, S., Yabuki, S., Yanagisawa, F. and Motoyama, R. 2002. The chemical and strontium isotope composition of atmospheric aerosols over Japan: the contribution of long-range-transported Asian dust (Kosa). *Atmos. Environ.* **36**, 5159–5175.

Kasper, A. and Puxbaum, H. 1998. Seasonal variation of SO_2, HNO_3, NH_3, and selected aerosol components at Sonnblick (3106 m a.s.l.). *Atmos. Environ.* **32**, 3925–3939.

Kaufman, Y., Tanre, D. and Boucher, O. 2002. A satellite view of aerosols in the climate system. *Nature* **419**, 215–223.

Kawamura, K. and Kaplan, I. R. 1987. Motor exhaust emissions as a primary source for dicarboxylic acids in Los Angeles ambient air. *Environ. Sci. Technol.* **21**, 105–110.

Kido, M., Osada, K., Matsunaga, K. and Iwasaka, Y. 2001a. Diurnal variation of ionic aerosol species and water-soluble gas concentrations at a high elevation site in the Japan. *J. Geophys. Res.* **106**, 17335–17345.

Kido, M., Osada, K., Matsunaga, K. and Iwasaka, Y. 2001b. Temporal change in ammonium/sulfate ratios for free tropospheric aerosols from early winter to spring at a high elevation site in the Japanese Alps. *J. Environ. Chem.* **11**, 33–41.

Kline, J., Huebert, B., Howell, S., Blomquist, B., Zhuang, J. and co-authors. 2004. Aerosol composition and size versus altitude measured from a C-130 during ACE-Asia. *J. Geophys. Res.* **109**, doi:10.1029/2004JD004540.

Kurosaki, Y. and Mikami, M. 2003. Recent frequent events and their relation to surface wind in East Asia. *Geophys. Res. Lett.* **30**, doi: 10.1029/2003GL017261.

Lee, G., Merrill, J. T. and Huebert, B. J. 1994. Variation of free tropospheric total nitrate at Mauna Loa observatory, Hawaii. *J. Geophys. Res.* **99**, 12821–12831.

Mendonca, B. G. 1969. Local wind circulation on the slopes of Mauna Loa. *J. Appl. Meteorol.* **8**, 533–541.

Mori, I., Iwasaka, Y., Matsunaga, K., Hayashi, M. and Nishikawa, M. 1999. Chemical characteristics of free tropospheric aerosols over the Japan Sea coast: aircraft-borne measurements. *Atmos. Environ.* **33**, 601–609.

Mukai, H., Ambe, Y. and Shibata, K. 1990. Long-term variation of chemical composition of atmospheric aerosol on the Oki Islands in the sea of Japan. *Atmos. Environ.* **24A**, 1379–1390.

Narukawa, M., Kawamura, K., Takeuchi, N. and Nakajima, T. 1999. Distribution of dicarboxylic acids and carbon isotopic compositions in aerosols from 1997 Indonesian forest fires. *Geophys. Res. Lett.* **26**, 3101–3104.

Nishikawa, M., Kanamori, S., Kanamori, N. and Mizoguchi, T. 1991. Kosa aerosol as eolian carrier of anthropogenic materials. *Sci. Tot. Environ.* **107**, 13–27.

Nishita, C., Osada, K., Matsunaga, K. and Iwasaka, Y. 2007. Number-size distributions of free tropospheric aerosol particles at Mt. Norikura, Japan: effects of precipitation and air-mass transportation pathways. *J. Geophys. Res.* doi:10.1029/2002JD007969.

Nyeki, S., Baltensperger, U., Colbeck, I., Jost, D. T., Weingartner, E., and co-authors. 1998. The Jungfraujoch high-alpine research station (3454 m) as a background clean continental site for the measurement of aerosol parameters. *J. Geophys. Res.* **103**, 6097–6107.

Ohta, S. and Okita, T. 1990. A chemical characterization of atmospheric aerosol in Sapporo. *Atmos. Environ.* **24A**, 815–822.

Ooki, A. and Uematsu, M. 2005. Chemical interaction between mineral dust particles and acid gases during Asian dust events. *J. Geophys. Res.* **110**, doi:10.1029/2004JD004737.

Osada, K., Kido, M., Nishita, C., Matsunaga, K., Iwasaka, Y. and co-authors. 2002. Changes in ionic constituents of free tropospheric aerosol particles obtained at Mt. Norikura (2770 m asl), central Japan, during the Shurin period in 2000. *Atmos. Environ.* **36**, 5469–5477.

Osada, K., Kido, M., Iida, H., Matsunaga, K., Iwasaka, Y. and co-authors. 2003. Seasonal variation of free tropospheric aerosol particles at Mt. Tateyama, central Japan. *J. Geophys. Res.* **108**, doi:10.1029/2003JD003544.

Perry, K., Cahill, T. A., Schnell, R. C. and Harris, J. M. 1999. Long-range transport of anthropogenic aerosols to the National Oceanic and Atmospheric Administration baseline station at Mauna Loa Observatory, Hawaii. *J. Geophys. Res.* **104**, 18521–18533.

Preunkert, S., Wagenbach, D. and Legrand, M. 2002. Improvement and characterization of an automatic aerosol sampler for remote (glacier) sites. *Atmos. Environ.* **36**, 1221–1232.

Pye, K. 1987. *Aeolian dust and dust deposits*. Academic Press Inc., San Diego, pp. 334.

Sakai, T., Shibata, T., Kwon, S.-A., Kim, Y.-K., Tamura, K. and co-authors. 2000. Free tropospheric aerosol backscatter, depolarization ratio, and relative humidity measured with the Raman lidar at Nagoya in 1994–1997: contributions of aerosols from the Asian continent and the Pacific Ocean. *Atmos. Environ.* **34**, 431–442.

Satsumabayashi, H., Kawamura, M., Katsuno, T., Futaki, K., Murao, K. and co-authors. 2004. Effects of volcanic effluents on airborne particles and precipitation in central Japan. *J. Geophys. Res.* **109**, doi:10.1029/JD2003 JD004204.

Seibert, P., Kromp-kolb, H., Kasper, A., Kalina, M., Puxbaum, H. and co-authors. 1998. Transport of polluted boundary layer air from the Po Valley to high-alpine sites. *Atmos. Environ.* **32**, 3953–3965.

Seinfeld, J. H. and Pandis, S. N. 2006. *Atmospheric Chemistry and Physics* 2nd Edition. John Wiley & Sons, New Jersey, 1203.

Streets, D. G., Bond, T. C., Carmichael, G. R., Fernandes, S. D., Fu, Q., He, D. and co-authors. 2003. An inventory of gaseous and primary aerosol emissions in Asia in the year 2000. *J. Geophys. Res.* **108**, doi: 10.1029/2002JD003093.

Stull, R. B. 2000. Boundary layers. In: *Meteorology for Scientist and Engineers* 2nd Edition. (ed.R. B. Stull). Brooks/Cole, California, 65–64.

Sun, J., Zhang, M. and Liu, T. 2001. Spatial and temporal characteristics of dust storms in China and its surrounding regions, 1960–1999: relations to source area and climate. *J. Geophys. Res.* **106**, 10325–10333.

Suzuki, T. and Tsunogai, S. 1988. Origin of calcium in aerosols over the western north Pacific. *J. Atmos. Chem.* **6**, 363–374.

Uematsu, M., Duce, R. A., Prospero, J. M., Chen, L., Merrill, J., and co-authors. 1983. Transport of mineral aerosols from Asia over the north Pacific Ocean. *J. Geophys. Res.* **88**, 5343–5352.

Uematsu, M., Yoshikawa, A., Muraki, H., Arao, K. and Uno, I. 2002. Transport of mineral and anthropogenic aerosols during a Kosa event over East Asia. *J. Geophys. Res*. **107**, doi: 10.1029/2001 JD000333.

Warneck, P. 1999. *Chemistry of the Natural Atmosphere*. 2nd Edition. Academic Press Inc., San Diego, pp. 927.

Warneck, P. 2003. In-cloud chemistry opens pathway to the formation of oxalic acid in the marine atmosphere. *Atmos. Environ*. **37**, 2423–2427.

Warneck, P. 2005. Multi-phase chemistry of C2 and C3 organic compounds in the marine atmosphere. *J. Atmos. Chem.* **51**, 119–159.

Whiteman, C. D. 2000. *Mountain Meteorology*. Oxford University Press, Oxford, pp. 355.

Wilson, T. R. S. 1975. Salinity and the major elements of seawater. In: *Chemical Oceanography*. Volume 1. (eds J. P. Riley and G. Skirrow), Academic Press Inc., San Diego, 365–413.

Yoon, S.-C., Kim, S.-W., Kim, J., Sohn, B.-J., Jefferson, A. and co-authors. 2006. Enhanced water vapor in the Asian dust layer: entrainment processes and implication for aerosol optical properties. *Atmos. Environ*. **40**, 2409–2421.